Earth Sciences
2015; 4(2): 80-88
Published online April 9, 2015 (http://www.sciencepublishinggroup.com/j/earth)
doi: 10.11648/j.earth.20150402.13
ISSN: 2328-5974 (Print); ISSN: 2328-5982 (Online)

Global Mid-Ocean Ridges Mantle Tomography Profiles

Desiderius Cyril Patrick Masalu

University of Dar es Salaam, Institute of Marine Sciences, Zanzibar, Tanzania

Email address:
masalu@ims.udsm.ac.tz (D. C. P. Masalu)

To cite this article:
Desiderius Cyril Patrick Masalu. Global Mid-Ocean Ridges Mantle Tomography Profiles. *Earth Sciences*. Vol. 4, No. 2, 2015, pp. 80-88.
doi: 10.11648/j.earth.20150402.13

Abstract: We have studied mantle tomography profiles of global mid-ocean ridges to investigate their depth of origin and other characteristics. The Mid-Atlantic and the South West Indian Ridges are deep rooted ridges that extend as far down in the mantle to 250-300 km. The Central Indian Ridge, South East Indian Ridge, Antarctica Nazca, Pacific Antarctica, Pacific Nazca and Juan de Fuca are shallow rooted ridges that extend down in the mantle only to 100 km. The deep rooted ridges appear to be characterized by a weak low velocity ridge anomaly while the shallow rooted ridges are characterized by strong low velocity ridge anomaly. This may be due to the variations of the geochemistry of the ridges due to the fractionation process during magma ascent. Furthermore, despite the three ridges that make the Indian Rodriguez Triple Junction having different characteristics, all the three sections of the ridges that make the Triple Junction are characterized by strong low velocity ridge anomaly and extended down to only 100 km. This is particularly typical for the length of nine to ten degrees from the Triple Junction which makes it appear as an independent system.

Keywords: Mid-Ocean Ridges, Mantle Tomography, Hotspot, Triple Junction

1. Introduction

Global tomography is a technique which involves the interpretation of observed seismic wave field in terms of seismic properties at depth to image the interior of the solid earth [1, 2]. The technique emerged about three decades ago. Tomography is used in global imaging to study the interior of the earth for various geophysical investigations, for example, mantle convection [3], mantle heterogeneities [4, 5], plumes [6], detection of subducted and folded lithosphere [7] and so on. Several digital global mantle tomography models have been developed and published [e.g. 5, 8-12]. These models are used to study the earth's interior and investigate geophysical processes.

Mantle profiles along global mid-ocean ridges were investigated in order to study the depth of origin of mid-ocean ridges and other characteristics of the profiles. This information would assist in the detail understanding and/or quantification of the various studies on mid-ocean ridges such as mid-ocean ridge basalt chemical systematics [e.g. 13, 14], correlation with kinematic parameters [e.g., 15], mid-ocean ridge tectonics [e.g., 16-18] and other geophysical and geochemical studies.

2. Methods

Several available models of global mantle tomography [5, 8-12] were assessed for use in this study. With the exception of the Zhang & Tanimoto [12] model all other models were obtained from the REM webpage [19]. However, all these models except only for the Zhang & Tanimoto [12] model were found to have no suitable resolutions for this study which focuses on the top 600 km of the earth. Models from the REM webpage [19] are 4 by 4 degrees maps at depth intervals ranging from 89 to 130 km in the top 650 km of the earth. These models have trouble imaging narrow, shallow features like mid-ocean ridges. On the other hand, the Zhang & Tanimoto [12] model is a 2 by 2 degrees horizontally and for the first 90 km has four depth intervals ranging from 8 to 28 km starting at 10 km depth, and from 90 km to 650 km depth intervals of 20 km. Furthermore, this model uses surface waves and so it is better able to resolve shallow structures/features. The Zhang & Tanimoto [12] model was therefore chosen and used in this study as it offered relatively better resolution both horizontally and vertically that could image mid-ocean ridges. A Fortran program was coded to read the Zhang & Tanimoto [12] model and output the tomographic profile along a given segment of a mid ocean ridge. The mid-ocean ridge mantle profiles were plotted using the GMT

system [20-25]. Hotspots were also incorporated (Fig. 1) in order to study how they might be interacting and influence the depth of origin of mid-ocean ridges and the characteristics of the profiles.

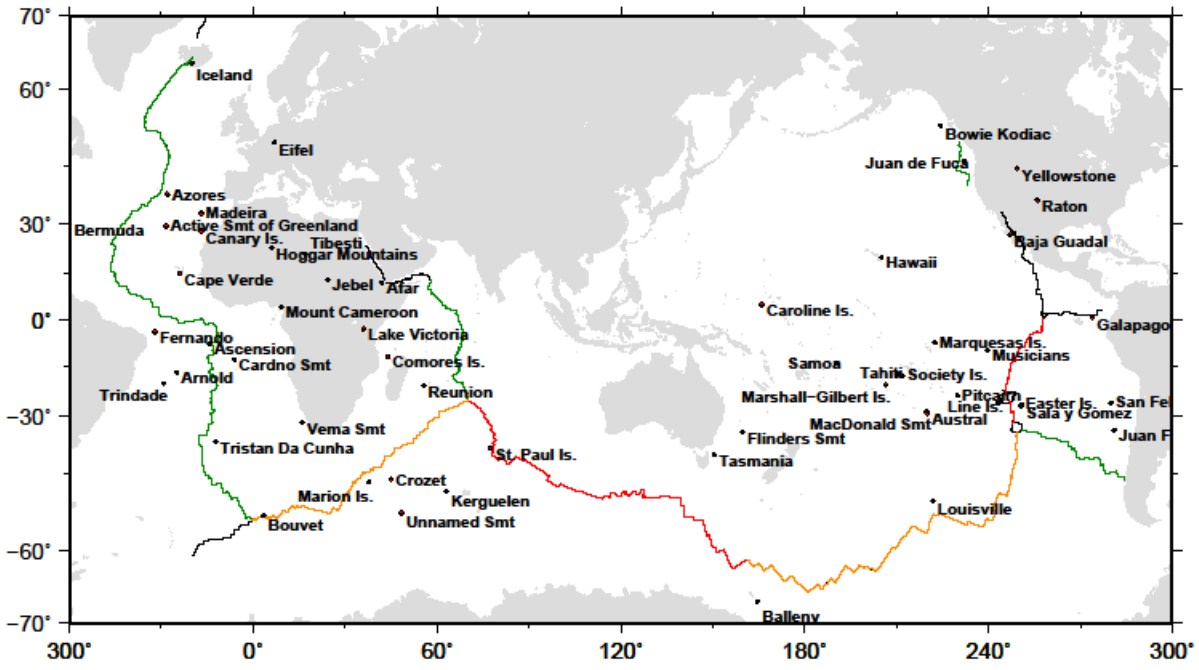

Figure 1. *Global mid-ocean ridge system and hotspot distribution. Colors indicate the different ridges studied in this work.*

3. Results

Eight mantle tomography profiles along global mid-ocean ridges were plotted and studied. The profiles were found to exhibit different features and characteristics. Several profiles revealed existence of low velocity areas that were oval or round in shape below the mid-ocean ridge signal. In some cases layers of low velocity signal were also identified. Some of these features were located very close to the ridge signal and could mislead the interpretation of the depth of origin of the ridge. Furthermore, in some cases features were found to be totally merged/integrated with the ridge signal and appeared as one continuous feature, and were interpreted that way.

3.1. The Central Indian Ridge (CIR)

The CIR is characterized by a weak low velocity ridge anomaly (LVRA) signal which extends as a continuous feature down to 80 - 100 km (Fig. 2). Three low velocity anomaly (LVA) areas that indicate hotter parts of the mantle than surrounding exist below the LVRA at 5°N, 8°S and 22°S. The LVAs at 8°S and 22°S appear to be connected by a gently slanting LVA. Furthermore, the southern LVA appears to be connected to the CIR's LVRA. No hotspot is located on or close to the section of the ridge that was studied.

3.2. The South East Indian Ridge (SEIR)

The SEIR (Fig. 3) is characterized by a strong and clear LVRA that generally extends as a continuous feature down to 100 km. However, at several locations the LVRA appear to extend down beyond 100 km as follows: firstly, between 78°E – 94°E there is a relatively LVA that appears to be loosely connected to the LVRA. This LVA extends down as a continuous feature to 350 – 400 km. This can be attributed to the presence of the St. Paul Island hotspot which is located very close to the SEIR at about 77°E. Secondly, from 128°E eastward the strong LVRA extends further down to about 180 km at 145°E and at 150°E the anomaly extends further down to about 300 km in a shape like a vertical conduit. The vertical conduit-like LVA appears to be connected to a LVA at 220 and 350 km that extends eastward. This may indicate that the section of the SEIR between 130°E and 150°E may be supplied with magma from deeper mantle through the vertical conduit-like LVA. However, there are no hotspots around this area. Furthermore, the LVRA of the SEIR appears to thin out between 110°E – 125°E. This location corresponds with the Australia-Antarctica-Discordance.

3.3. The South West Indian Ridge (SWIR)

The SWIR generally has a weak LVRA which is segmented at several locations and that extends down to about 100 km (Fig. 4). However, from 61°E to 70°E the LVRA has a very strong signal that looks very much similar to the LVRA signals observed on the SEIR and CIR near the Indian Rodriguez Triple Junction.

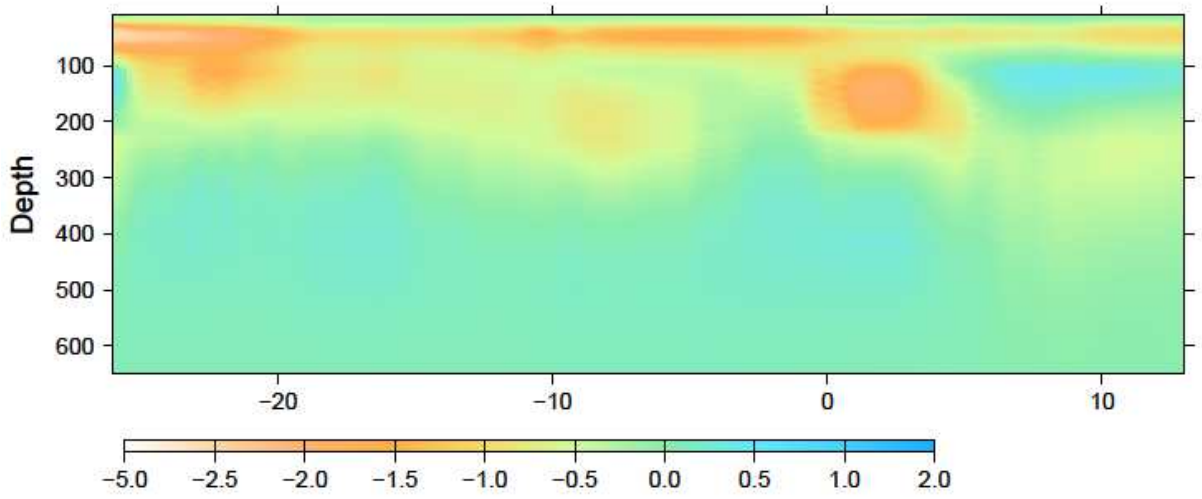

Figure 2. *Mantle profile beneath the Central Indian Ridge. Depth in Km. Vertical arrows indicate relative locations of hotspots. Red arrows indicate hotspot(s) located on or very close to the ridge while blue arrows indicate hotspot(s) located a bit far from the ridge.*

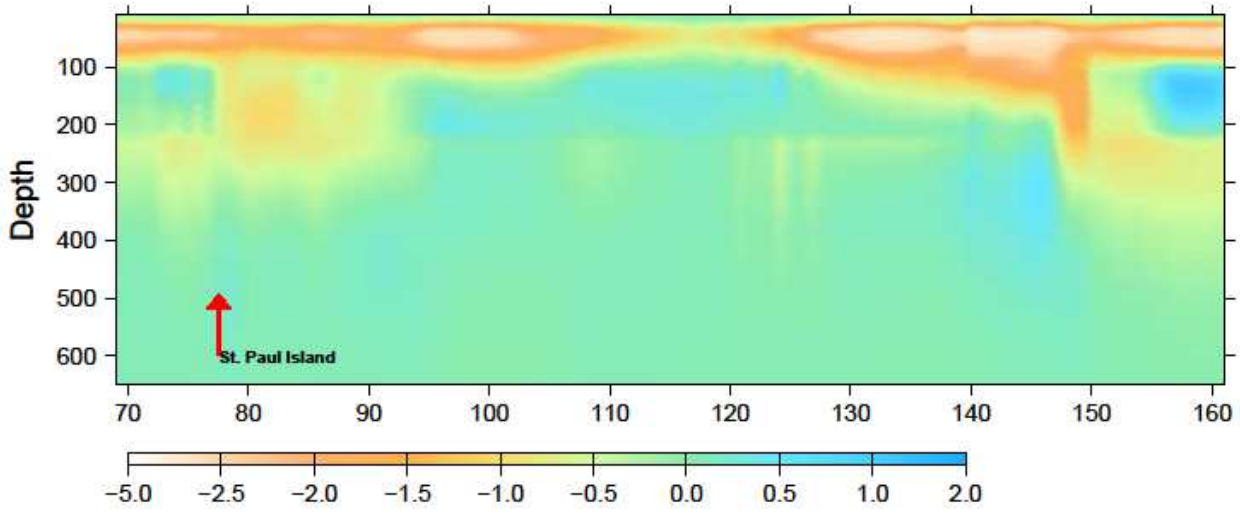

Figure 3. *Mantle profile beneath the Southeast Indian Ridge. Other panels as in Fig. 2.*

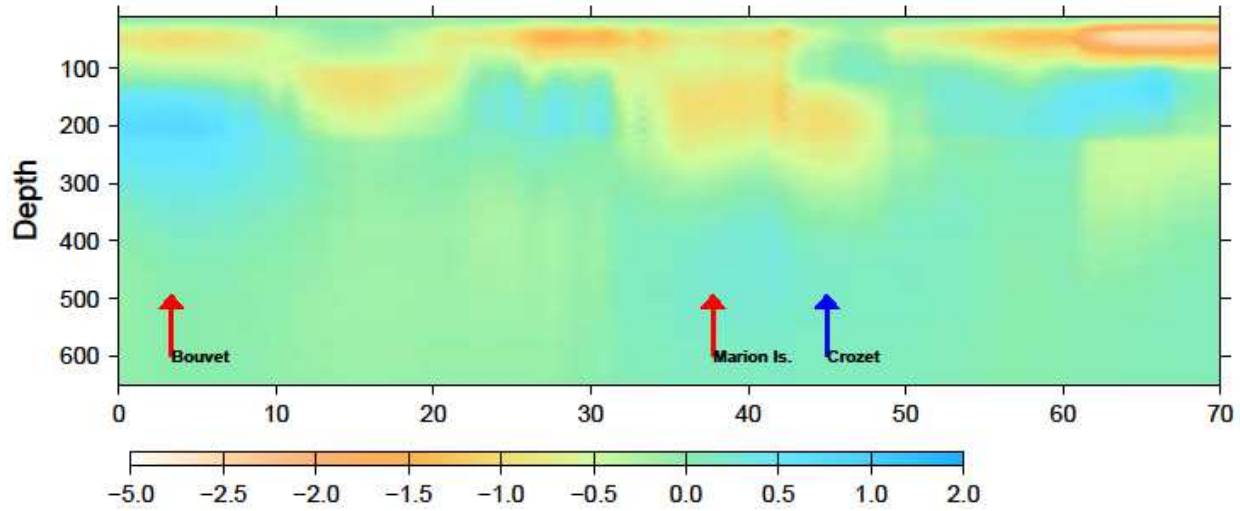

Figure 4. *Mantle profile beneath the Southwest Indian Ridge. Other panels as in Fig. 2.*

West of 61°E three anomalously hotter mantle areas are observed as follows: between 11°E and 22°E and 110 km and

220 km, between 32°E and 42°E and 100 km and 250 km, and between 42°E and 52°E and 120 km and 300 km.

Several hotspots exist along the SWIR. The Bouvet hotspot is located at 3°E on/very close to the ridge but seems to have no any influence to the ridge anomaly. On the other hand, two hotspots, the Marion Island which is located very close to the ridge at 37°E and the Crozet which is located a bit far from the ridge at 45°E, may be related to the LVA areas between 32°E - 52°E and 42°E - 52°E. However, the LVRA and the LVA due to the influence of the hotspots do not appear to be fully merged into a single continuous feature.

3.4. The Mid-Atlantic Ridge (MAR)

The MAR is characterized by both a strong and weak LVRA which is segmented at several locations (Fig. 5). The MAR interacts with six hotspots four of which are located on or very close to the ridge. The LVRA of the MAR and presumably the LVAs due to the presence of hotspots appear to be fully merged into a one continuous feature which makes the MAR profile peculiar from the others. From the south, the MAR LVRA increases in depth of extent from 110 km at 55°S to about 250 km at 37°S which coincides with the closely located Tristan da Cunha hotspot. The LVRA then decreases northward to 120 km at 20°S and reaches 100 km at 20°N. The Cardino hotspot located a bit far from the ridge at 13°S and the Ascension hotspot located very close to the ridge at 8°S may influence the extent of the LVRA down to 250 km between 15°S and 0°.

The MAR's LVRA extends to a depth of 270 km between 25°N and 40°N. The two deepest LVRA points on this section coincide with the locations of the Active Seamount of Greenland hotspot which is located a bit far from the ridge and the Azores hotspot which is located very close/on the ridge. This suggests that the two hotspots may interact with and influence the extent of the LVRA. At north, from 55°N northward, the LVRA extends down to 235 km and coincides with the location of the Iceland hotspot located at 66°N.

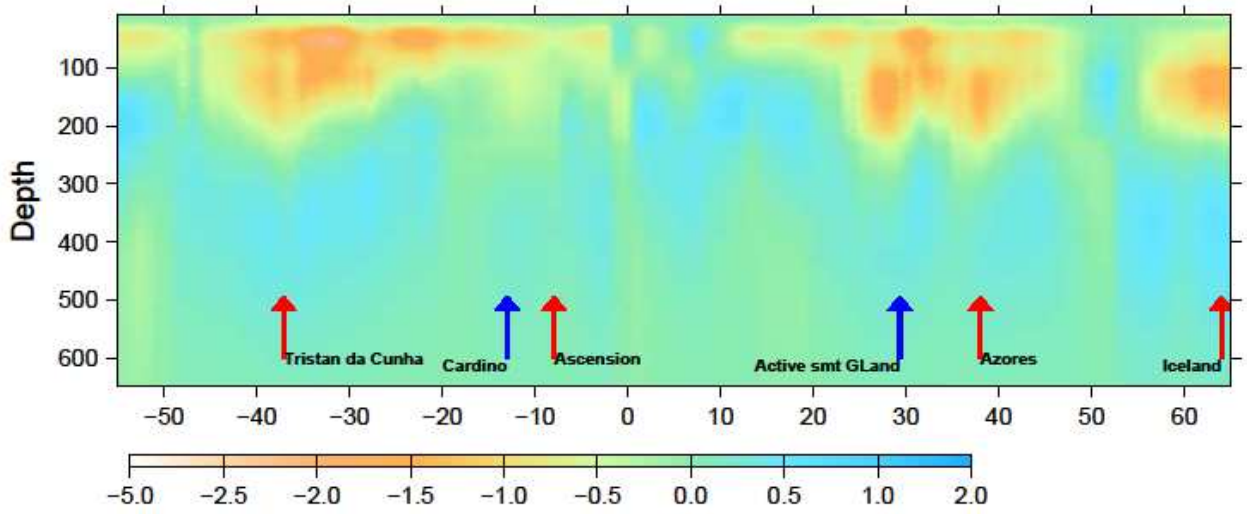

Figure 5. *Mantle profile beneath the Mid-Atlantic Ridge. Other panels as in Fig. 2.*

3.5. The Pacific–Antarctica Ridge (PacAnt)

The PacAnt (Fig. 6) has a very strong clear and non-segmented LVRA that extends down to 100 km depth almost throughout the ridge. The LVRA is underlain by a layer of high velocity anomaly that extends from 100 to 220 km. Below this layer there is LVA material/layer, and at depths between 200 and 400 km between 176°E and 196°E there is a strong LVA material emplaced in an oval shape that indicates hotter mantle than surrounding. The ridge appears to interact with the mantle below the high velocity layer that underlies the LVRA particularly between 195°E and 220°E and between 230°E and 245°E. These LVAs may be the influence of the Louisville hotspot which is located close to the ridge at 222°E. On the other hand, the Balleny hotspot which is located a bit far from the ridge does not appear to have any influence.

3.6. The Pacific-Nazca Ridge (PacNaz)

The PacNaz ridge has a very strong LVRA that mainly extends down to 100 km (Fig. 7). Two areas with anomalously hot mantle exist at 3°S and 8°S at a depth between 100 and 300 km. The two anomalously hot areas are connected by a layer of LVA that lies below the LRVA at about 250 km. This layer is about 20 – 100 km in thickness and extends from 23°S northward. The northern hot mantle parcel appears to interact with the ridge directly. Two hotpots i.e., Easter and Sala y Gomez are located very close each other and to the ridge at 27°S, and another hotspot, Musician, is located a bit far from the ridge at 10°S. The Musician hotspot appears to have no influence on the LVRA of the PacNaz and the probable correlation of this hotspot and the two anomalously hot mantle parts can not be ascertained by this study. On the other hand, the Easter and Sala y Gomez hotspots may have some influence on the LVRA. The LVRA at the location of the two hotspots extends to 200 km.

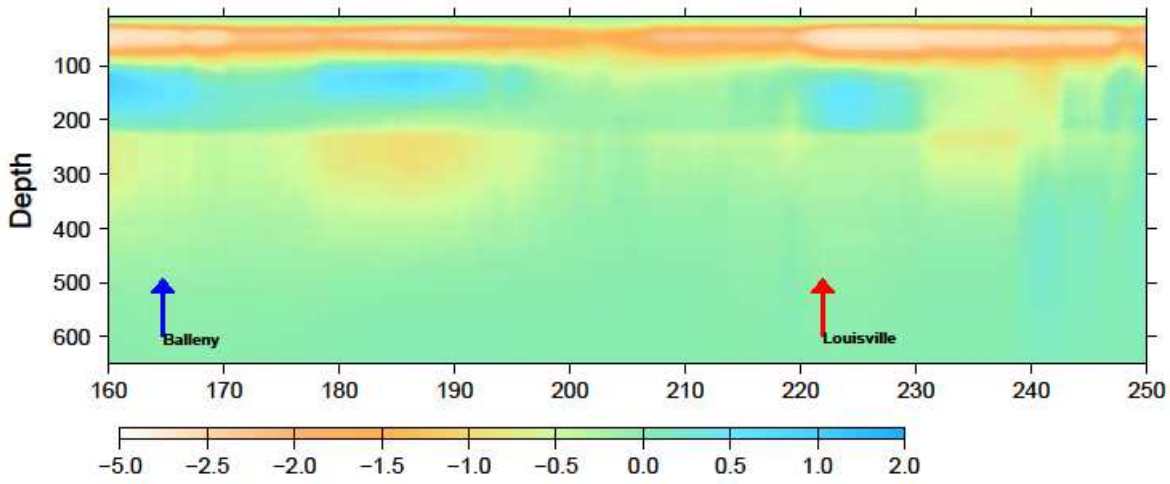

Figure 6. *Mantle profile beneath the Pacific-Antarctica Ridge. Other panels as in Fig. 2.*

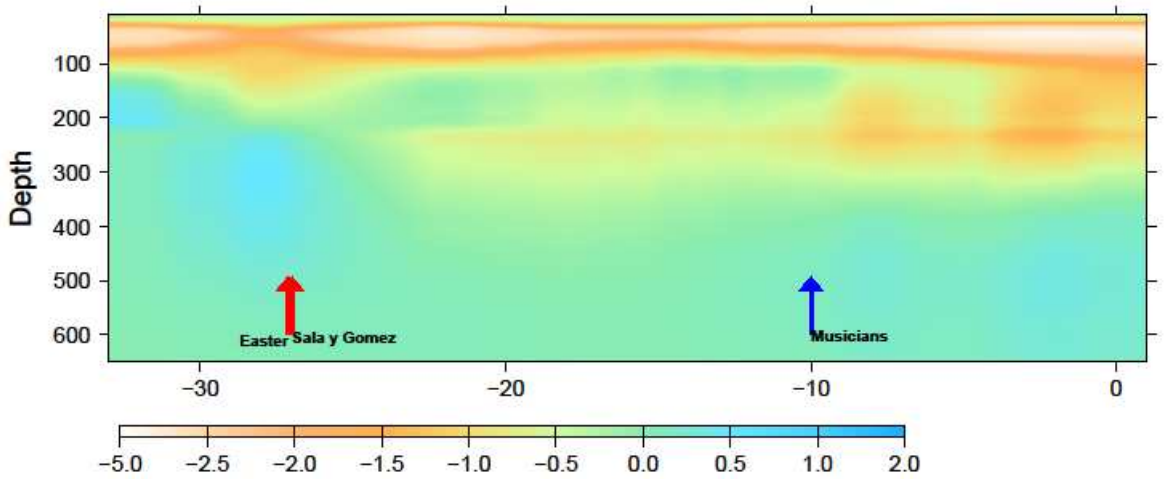

Figure 7. *Mantle profile beneath the Pacific-Nazca Ridge. Other panels as in Fig. 2.*

3.7. The Antarctic-Nazca Ridge (AntNaz)

The AntNaz ridge has a LVRA that is characterized by both strong and weak signals which extends down to 100 km. In particular, the LVRA between 250°E – 258°E is strong and thick than the rest of the ridge. The strong LVRA signal on the south of this ridge may be related to the triple junction this ridge forms with the PacAnt and PacNaz ridges. The AntNaz ridge's anomaly appears to extend further down to 250 and 300 km as a weak LVRA (Fig. 8). However, a careful investigation of the AntNaz profile reveals that two small anomalously hot mantle parts may exist at 282°E and 277°E between 100 and 200 km, and similarly another relatively large but weak in signal hot mantle may exists at 267°E between 200 and 300 km. Three hotspots exist that are located a bit far from the ridge. These are the Easter, Sala y Gomez and Juan Fernandez hotspots. Investigation of the LVRA indicates that the location of the Juan Fernandez hotspot corresponds with location of the two small hot mantle parts at north suggesting that the Juan Fernandez hotspot may interact with the ridge. The other two hotspots seem to have no any influence to the AntNaz.

3.8. The Juan de Fuca Ridge (Juan)

The Juan de Fuca ridge (Fig. 9) is characterized by a strong and continuous LVRA which extends as a continuous feature down to 100 km. A strong LVA layer located between 100 and 220 km at the southern end appears to join Juan's LVRA between 41°N and 45°N. The layer could be the extension of the LVA layer situated at about 250 km below the PacNaz's LVRA that extends for more than three quarters of the PacNaz ridge length from about 25°S northwards (Fig. 7). Below the Juan LVRA from 45°N to 50°N a weak LVA appears to extend down to 650 km. This could be related to the Juan de Fuca hotspot that lies very close to the ridge.

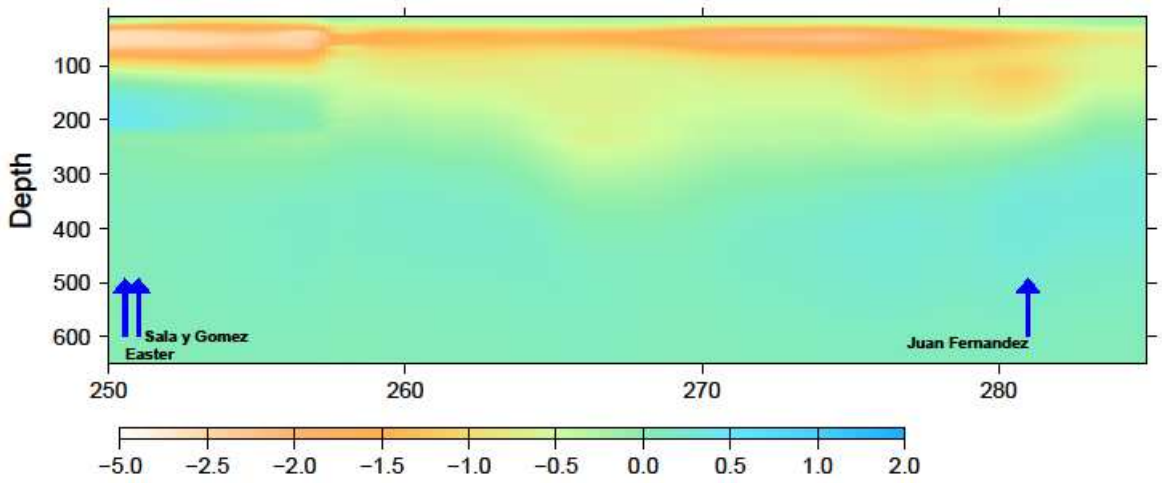

Figure 8. *Mantle profile beneath the Antarctica-Nazca Ridge. Other panels as in Fig. 2.*

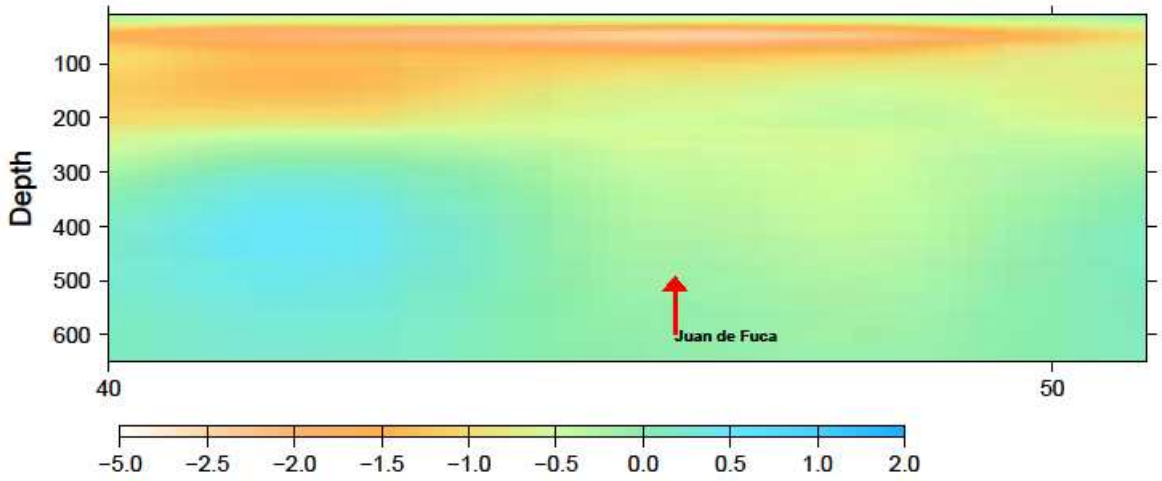

Figure 9. *Mantle profile beneath the Juan de Fuca Ridge. Other panels as in Fig. 2.*

4. Discussion

The mantle tomography profiles of the eight mid-ocean ridges investigated in this study reveal several important results and information. Based on the study of the profiles the MAR appears to be the only deep rooted ridge that extends as far down in the mantle to 250 km. The MAR profile is particularly peculiar in that the LVRA and the LVA below the LVRA appear to be fully merged into a single continuous feature. All the other ridges have LVRAs extending only down to 100 km [12]. However, several of the shallow rooted ridges appeared to have LVA features in their profiles that extended further deeper than the general ridge depth of extent as has been detailed in the previous section and as indicated in Table 1. Su et al. [26] concluded that the MAR, Pacific-Antarctic ridge (PacAnt), SWIR, and Carlsberg ridges, were deeper rooted ridges extending down to 400 – 600 km. However, the ridge profile for the PacAnt (Fig. 6.) clearly shows that that ridge is of shallow origin extending only to 100 km depth. On the other hand the SWIR appears to have deeper reaching LVA features that are however not very well fully merged with the LVRA of the SWIR. This may require other methods/approach to verify whether or not the MAR interacts with the deeper mantle to ascertain its deep origin.

Table 1. *Depths of origin of global mid-ocean ridges. Depths in parenthesis are due to some small scale sections/features of the ridge*

S/No	Mid-ocean ridge	Depth of origin (km)
1	Central Indian (CIR)	100 (300)
2	South East Indian (SEIR)	100 (180)
3	South West Indian (SWIR)	100 (300)
4	Mid-Atlantic (MAR)	250
5	Pacific – Antarctica (PacAnt)	100
6	Pacific – Nazca (PacNaz)	100 (300)
7	Antarctica – Nazca (AntNaz)	100 (300)
8	Juan de Fuca (Juan)	100 (200)

We note here that the actual depth of origin of mid-ocean ridges as indicated by Su et al. [26] differ from that observed in this study based on the Zhang & Tanimoto [12] model. This could be attributed to the differences of the two models particularly that the Zhang & Tanimoto [12] model uses surface waves (shear waves) while Su et al. [26] used SS waves. This discrepancy can not be resolved by this study.

We show in Fig. 10 Dy/Yb ratios of mid-ocean ridges in this study except only for the AntNaz ridge for which we could not

get the data. Higher Dy/Yb ratios indicate melt originating at greater mantle depths owing to the presence of residual garnet [15]. Disregarding points that are clearly outlier, the Dy/Yb ratio ranges vary as follows: SWIR, 1.5 – 2.15; SEIR, 1.57 – 1.83; CIR, 1.59 – 1.71; MAR, 1.2 – 2.75; SMAR, 1.4 – 2.41; PacAnt, 1.35 – 1.77; PacNaz, 1.47 – 2.44; and Juan, 1.36 – 1.87. Based on these results the MAR, SWIR and PacNaz have the highest upper ranges of the Dy/Yb ratios indicating they are sampling deeper mantle than the other ridges. These results therefore confirm that the MAR is deep rooted and that the SWIR is interacting with the LVA features below it and thus may in deed be deep rooted too as observed by Su et al. [26]. Furthermore, these results indicate that the PacNaz ridge may also be interacting with the LVA features below it. These results also confirm that the rest of the mid-ocean ridges, although some have LVA features below them extending down deeper into the mantle, are of shallow origin.

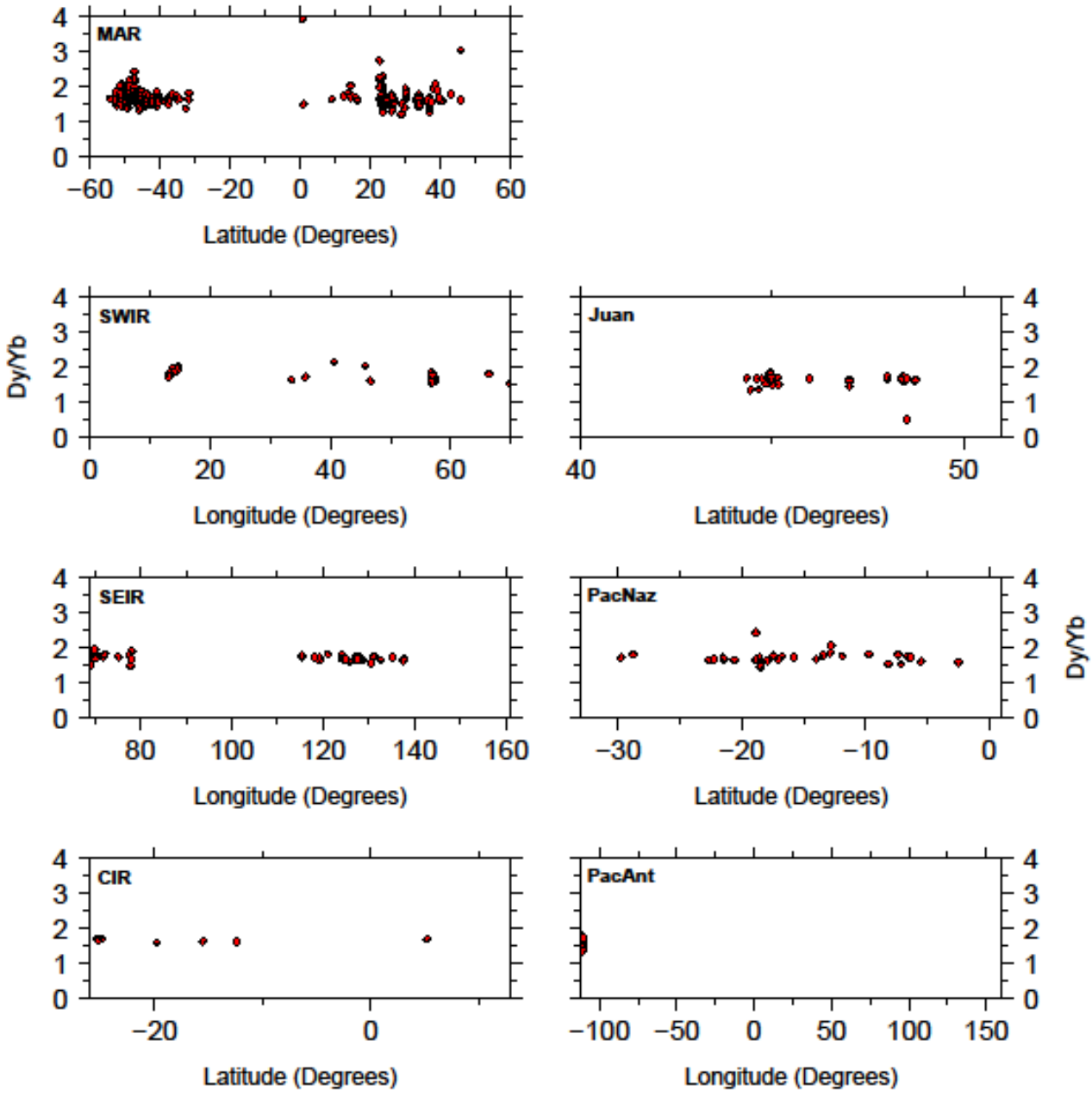

Figure 10. *Dy/Yb ration of mid-ocean ridges in this study.*

The mid-ocean ridges studied displayed varying characteristics of the strength of the LVRA signal that gets stronger the more the tomographic velocity gets smaller. Based on this the SEIR, PacAnt, PacNaz, AntNaz and Juan ridges were found to be characterized by strong LVRAs while the SWIR, CIR and MAR ridges were characterized by weak LVRAs. Based on the results of this study as discussed above, with the exception of the CIR only, ridges with stronger LVRAs appear to correspond to the shallow rooted ridges and those with weak LVRA correspond to the deep rooted ridges.

This observation suggests variations in the geochemistry of the ridges in the two groups in such a way their ability to propagate seismic signal is greatly influenced. Studies on the chemical systematics of global mid-ocean ridge basalts as it ascends has shown that it undergoes chemical fractionation to an extent that depends on its depth of origin [13, 14]. Hotter mantle material from deeper depths intersects the solidus at greater depth and produces a taller melting column, leading to greater mean pressures and extent of melting whereas cooler mantle material from shallow depth intersects the solidus at shallower depth and produces a shorter melting column, leading to lower mean pressures and extent of melting [13, 14].

Based on the study of the strength of the LVRA signals this study also imaged the Indian Rodriguez Triple Junction (RTJ). All the three sections of the ridges that make the RTJ are characterized by strong LVRA and extended down to only 100 km. In particular, this seems to be typical for the 9 to 10 degrees of length from the triple junction along each ridge section. The RTJ therefore appears to behave as and independent system connected to the three ridges. We also did similar investigations on the other Triple Junctions that were fully or partially covered in this study, i.e., the PacAnt-PacNaz-AntNaz and MAR-SWIR-SAmAnt, to investigate any similarities in characteristics with the RTJ. The PacAnt-PacNaz-Ant triple junction was found to have characteristics very similar to the RTJ. The two triple junctions are ridge-ridge-ridge (RRR) triple junctions and are characterized by strong LVRAs signals. However, the MAR-SWIR-SAmAnt triple junction which is a ridge-fault-ridge (RFR) was characterized by weak signal of the LVRAs. We therefore suggest that RRR triple junctions may be characterized by strong LVRAs and all other types of triple junctions by weak LVRA. Further studies are needed to verify this observation and other characteristics of triple junctions within this context.

The ridge profiles investigated in this study reveal various interactions of hotspots and the mid-ocean ridges. Some hotspots that were located on or very close to the ridges appeared to have no influence/interaction with the ridges. An example for this is the Bouvet hotspot that is located on the SWIR. On the other hand, some hotspots that were located a bit far from the mid-ocean ridges appeared to interact with the ridges; examples are the Juan Fernandez hotspot and the AntNaz, the Louisville hotspot and the PacAnt, and the Juan de Fuca hotspot the Juan. The interaction between mid-ocean ridges and hotspots has been documented in details elsewhere [27].

5. Conclusion

Based on the current study of global mid-ocean ridge mantle tomography profiles and trace-elements chemistry, the Mid-Atlantic Ridge and the South West Indian Ridge are deep rooted ridges that extend as far down in the mantle to 250-300 km. The rest of the ridges are shallow rooted ridges that extend down in the mantle only to 100 km. Several ridges have various features of low velocity anomaly areas below them but most of them are not connected to the ridge's low velocity anomaly. However, the Mid-Atlantic Ridge has a peculiar profile in which the low velocity anomalies of the ridge and other low velocity areas below it have been fully merged into a one continuous feature. The Indian Rodriguez Triple Junction appears to have distinct characteristics for the length of nine to ten degrees from the Triple Junction. All the three sections of the ridges that make the Triple Junction are characterized by a strong low velocity ridge anomaly and extended down to only 100 km. This makes the Triple Junction appear as an independent system.

Acknowledgements

I thank the Japan Student Services Organization (JASSO) for offering me the JASSO Follow-up Research Fellowship to the University of Tokyo in 2006, during which this work was conceived and most if it done.

References

[1] A. M. Dziewonski, B. H. Hager and R. J. O'Connell "Large scale heterogeneities in the lower mantle" Journal of Geophysical Research, vol. 82, pp. 239-255, 1977.

[2] A. M. Dziewonski, "Mapping the lower mantle: determination of lateral heterogeneity in P velocity up to degree and order 6" Journal of Geophysical Research, vol 89, pp. 5929-5952, 1984.

[3] R. D. Van der Hilst, S. Widiyantoro and E. R. Engdahl "Evidence for deep mantle circulation from global tomography". Nature vol. 386, pp. 578-584, 1997.

[4] E. J. Garnero, T. Lay and A. McNamara "Implications of lower-mantle structural heterogeneity for existence and nature of whole-mantle plumes," in Plates, plumes and planetary processes of G. R. Foulger and D. M. Jurdy, pp. 79-101, doi: 10.1130/2007.2430(05), Geological Society of America Special Paper 430, 2007.

[5] J. Ritsema and H. J. van Heijst "Seismic imaging of structural heterogeneity in Earth's mantle: Evidence for large-scale mantle flow", Science Progress vol. 83, pp. 243-259, 2000.

[6] R. Montelli, G. Nolet, F. A. Dahlen, G. Masters, E. R. Engdahl and Shu-Huei Hung "Finite-frequency tomography reveals a variety of plumes in the mantle", Science, vol. 303, no. 5656, pp. 338-343, 2004.

[7] A. R. Hutko, T. Lay, E. J. Garnero and J. Revenaugh "Seismic detection of folded, subducted lithosphere at the core-mantle boundary", Nature, Vol. 441, no. 7091, pp. 333-336, 2006.

[8] Y. J. Gu and A. M. Dziewonski "Mantle Discontinuities and 3-D Tomographic Models". EOS Trans. AGU, vol. 80, F717, 1999.

[9] G. Masters, G. Laske, H. Bolton and A. Dziewonski "The Relative Behavior of Shear Velocity, Bulk Sound Speed, and Compressional Velocity in the Mantle: Implications for Chemical and Thermal Structure" in Earth's Deep Interior, of S. Karato, A. M. Forte, R. C. Liebermann, G . Masters and L. Stixrude, AGU Monograph 117, AGU, Washington D.C. 2000.

[10] C. Mégnin and B. Romanowicz "The three-dimensional shear velocity structure of the mantle from the inversion of body, surface and higher-mode waveforms", Geophysical Journal International, vol. 143, pp. 709-728, 2000.

[11] S. Grand "Global seismic tomography: a snapshot of convection in the Earth". GSA Today vol. 7, pp. 1-7, 1997.

[12] Y. S. Zhang and T. Tanimoto "Global Love wave phase velocity variation and its significance to plate tectonics", Physics and Earth Planetary Interior, vol. 66, pp. 160-202, 1991.

[13] E. M. Klein and C. H. Langmuir "Global Correlations of Ocean Ridge Basalt Chemistry with Axial Depth and Crustal Thickness", Journal of Geophysical Research, vol. 92, pp. 8089-8115, 1987.

[14] E. M. Klein and C. H. Langmuir "Local Versus Global Variations in Ocean Ridge Basalt Composition" A Reply. Journal of Geophysical Research, vol. 94, pp. 4241-4252, 1989.

[15] S. M. Carbotte, C. Small and K. Donnelly "The influence of ridge migration on the magmatic segmentation of mid-ocean ridges", Nature, vol. 429, pp. 743-746, 2004.

[16] D. C. P. Masalu "Absolute Migration of Pacific Basin Mid-Ocean Ridges Since 85 Ma and Tectonics in the Circum-Pacific Region", New Zealand Journal of Geology and Geophysics, vol. 54, no. 02, 249-254, DOI: 10.1080/00288306.2010.548768, 2010.

[17] D. C. P. Masalu "Mapping Absolute Migration of the Indian Triple Junction Since 75 Ma and Implication for its Evolution", The Open Geology Journal, vol. 4, pp. 58-61, doi: 10.2174/1874262901004010058, 2010.

[18] D. C. P. Masalu "Mapping absolute migration of global mid-ocean ridges since 80 Ma to Present", Earth Planets and Space vol. 59, pp. 1061-1066, 2007.

[19] REM webpage http://igppweb.ucsd.edu/~gabi/rem.html Accessed 16th March 2013.

[20] P. Wessel and W. H. F. Smith "Free software helps map and display data". EOS Transactions American Geophysical Union, vol72, no. 41, pp. 441-446, 1991.

[21] P. Wessel and W. H. F. Smith "New version of the Generic Mapping Tools released". EOS Transaction American Geophysical Union vol. 76, no. 33, pp. 329, 1995.

[22] P. Wessel and W. H. F. Smith "New version of the Generic Mapping Tools released" EOS Transaction American Geophysical Union, Electronic supplement, Available at http://www.agu.org/eos_elec/95154e.html, 1995.

[23] P. Wessel and W. H. F. Smith "New, improved version of Generic Mapping Tools released". EOS Transactions of American Geophysical Union, vol. 79, no. 47, pp. 579, 1998.

[24] W. H. F. Smith and P. Wessel "Gridding with continuous curvature splines in tension", Geophysics vol. 55, no. 3, pp. 293-305, 1990.

[25] GMT "GMT homepage", Available at http://gmt.soest.hawaii.edu/ Accessed September 2013.

[26] W. Su, R. L. Woodward and A. M. Dziewonski "Deep origin of mid-ocean ridge seismic velocity anomalies", Nature, vol. 360, pp. 149-152, 1992.

[27] Y. S. Zhang and T .Tanimoto "Ridges, hotspots and their interpretation as observed in seismic velocity maps", Nature, vol. 355, pp. 45-49, 1992.